Micro and Nano Systems Letters

LETTER Open Access

Development of platinum strain gauge based on Ni-Co metal substrate for smart catheter application

Yunho Kim, Jajin Kim and Yongdae Kim*

Abstract

Rapid diagnosis and treatment are required when blood clots build up in a blood vessel and clog up the vessel. This study proposes novel smart catheters that can simultaneously diagnose and treat blood vessel disease. This quick treatment increases survival probability and can prevent various complications. In the design of the smart catheters, Pt strain gauges can be used to measure the inside diameter of the vessel. This paper proposes a new fabrication process of the Pt strain gauges based on metal substrates made of Ni and Co alloy (referred to as "Ni-Co" in this paper). In the fabrication process, a Ni-Co thin film was deposited onto a silicon carrier wafer by electroplating and patterned into individual shapes by a liftoff process. Then, a multilayered Pt strain gauge consisting of insulation, adhesive layers, and Pt metallization was formed on the Ni-Co flexible substrate. Subsequently, the Pt strain gauges were peeled off from the carrier wafer by a new release process. To evaluate the performance of the strain gauges in terms of gauge factor and nonlinearity, tensile and compression tests were conducted by attaching Pt strain gauges to the constant stress beam.

Keywords: Smart catheter, Pt strain gauge, Ni-Co flexible substrate, Thrombosis, Vascular diseases

Introduction

Accumulation of blood clots in blood vessels causes thrombosis, which clogs the blood vessels. In the event of thrombosis, blood is not properly supplied to the organs, which can lead to stroke and acute myocardial infarction.

Common, conventional treatment methods for thrombosis carry out diagnosis and treatment sequentially, which requires a relatively long treatment time. The conventional method includes injecting a contrast medium into the patient for diagnosis when the patient is brought to the emergency room and monitoring the blood vessels using imaging equipment (e.g., CT, X-ray, or MRI). Through monitoring, blood clots are found and diagnosed. After diagnosis, additional contrast medium is typically injected to perform a catheter-using procedure, while viewing the blood vessels via the imaging equipment, or to facilitate blood flow through thrombosis removal surgery. For the catheter-using treatment of vascular disease, various kinds of catheters, featuring distal mechanisms that trigger motion such as ballooning or deploying several struts and subsequently removing blood clots, have been developed [1–4]. However, this existing process takes significant time because diagnosis and treatment are performed separately. Therefore, patient survival probability is reduced.

In our previous work, we proposed the design of an MEMS-based smart catheter that can simultaneously diagnose and treat vascular diseases [5]. The time taken to diagnose and treat thrombosis can be reduced by using a smart catheter. In the proposed smart catheter, a flexible structure in which a Pt strain gauge is formed on a Ni–Co thin film is applied to monitor blood vessels and remove blood clots. The Ni-Co thin film serves as a structural element as well as a

*Correspondence: ydkim@kiu.kr
Kyungil University, 50 Gamasilgil, Hayangeup, Gyeongsan, Gyeongbuk 38428, Republic of Korea

substrate. Ni-Co thin films have excellent mechanical strength and corrosion resistance, making them suitable as a structural material for smart catheters.

This study was carried out for a preliminary study to realize the smart catheter. A new fabrication process for Pt strain gauges was established based on a Ni-Co flexible substrate. Combining the micro fabrication technologies and the conventional electroplating technologies of Ni-Co, flexible micro devices, and smart catheters with a thickness of several micrometers with a very complex shape can be easily realized [6]. Because the Pt strain gauges are composed of a multilayered thin film in which adhesion, insulating, and Pt layers are formed on the Ni-Co substrate, the adhesion characteristics between the Ni-Co substrate and the upper layers are very important. Thus, the adhesion strength and cross-sectional structures of the thin films were investigated using a nano-scratch test and scanning electron microscopy (SEM), respectively. Subsequently, Pt strain gauges based on the Ni-Co flexible substrate were fabricated and their performance was evaluated by bonding on a constant stress beam made of stainless steel.

Concept of the smart catheter

Figure 1a shows a conceptual diagram of the proposed smart catheter, which allows the diagnosis and treatment of vascular diseases simultaneously, by monitoring the shape of the inside of the blood vessel. The catheter consists of the distal tip, outer shaft, inner shaft, probe structures, strain gauges formed on the probes, and a mesh structure for probe deployment and clot removal. The left and right sides of the mesh structure are attached to the digital tip and the outer shaft, respectively. Pulling inner shaft causes the mesh structure to expand in a direction perpendicular to the axis, which deploys the probes. After the deployment, the probes can monitor the internal shape of the blood vessel using the Pt strain gauges. When the catheter passes through the part where the internal diameter of the blood vessel has become smaller owing to the accumulation of blood clots, the changes in the electrical resistance of the strain gauges occurs. After locating the blood clots, the inner shaft is additionally pulled to further expand the mesh structure. Subsequently, the blood clots can be removed by pulling the catheter out of the patient's body for rapid treatment. The catheter can be implemented by attaching the multifunctional sheet based on Ni-Co flexible substrate throughout the distal tip and the outer shaft as shown in Fig. 1b).

Fabrication of Pt strain gauges

Fabrication process

Figure 2 shows the fabrication process of the thin films. SiO_2 with a thickness of 1 μm was deposited onto a silicon wafer via low-pressure chemical vapor deposition for electrical isolation from the silicon carrier wafer. Then, a Ti layer with a thickness of 200 Å was deposited by sputtering. Subsequently, a Cu layer with a thickness of 200 nm was deposited by sputtering as a seed layer for Ni-Co plating. Thereafter, a photoresist (PR) was coated and patterned to form a plating frame. In the electroplating process, because the PR-coated region is not electroplated, a Ni-Co thin film with the desired shape can be manufactured. Subsequently, 5 μm-thick Ni-Co was plated using electroplating equipment. After removing the PR, the Ti/Cu/Ni-Co thin film remained on the silicon carrier wafer on which SiO_2 was deposited (Fig. 2(5)). Then, a 200 Å thick Ti, as an adhesion improving layer, was deposited on the Ni-Co layer. Subsequently, SiO_2 and Si_3N_4 insulation layers with thicknesses of 700 nm and 300 nm, respectively, were deposited by plasma-enhanced chemical vapor deposition at 250 °C. Afterward, PR was coated and patterned, followed by deposition of a 40 nm-thick Ti adhesive layer and a 200 nm-thick Pt layer through sputtering. At this step, Pt metallization with individual shapes can be fabricated by lifting off the PR to form a Pt resistor and electrodes. Finally, after coating and patterning the PR, wet etching of SiO_2 and Si_3N_4 achieved the desired shape to produce flexible Pt strain gauges in which the adhesion, insulation layers, and Ti/Pt metallization formed on a Ni–Co metal thin film. Finally, the flexible Pt strain gauges based on the Ni-Co metal substrate were peeled off from the silicon carrier wafer using a new release process.

Figure 3 shows the release process of the strain gauge belt, where 5 Pt strain gauges are connected together by the connecting bridges, and the release tag is formed at one end of the strain gauge belt. During the release process, the edge of the release tag was separated by scribing with tweezers (Fig. 3(1) and (2)). Then, the belt was peeled off from the wafer by pulling the separated release tag with the tweezer (Fig. 3(3) and (4)).

Figure 4 shows the strain gauge belt peeled off from the Si carrier wafer. The thickness of the belt was approximately 6 μm, so that the belt was flexible. The individual Pt strain gauge based on the Ni-Co flexible film was separated by cutting the connecting bridge between the gauges and the release tag damaged during the release process with scissors, as shown in Fig. 4. The strain gauge consisted of multiple grids. The Pt strain gauge developed in this study had a width ($w = 20$ μm), gauge length ($l = 1.24$ mm), and number of grids ($n = 6$) and the total gauge length was 7.44 mm. In order to improve the

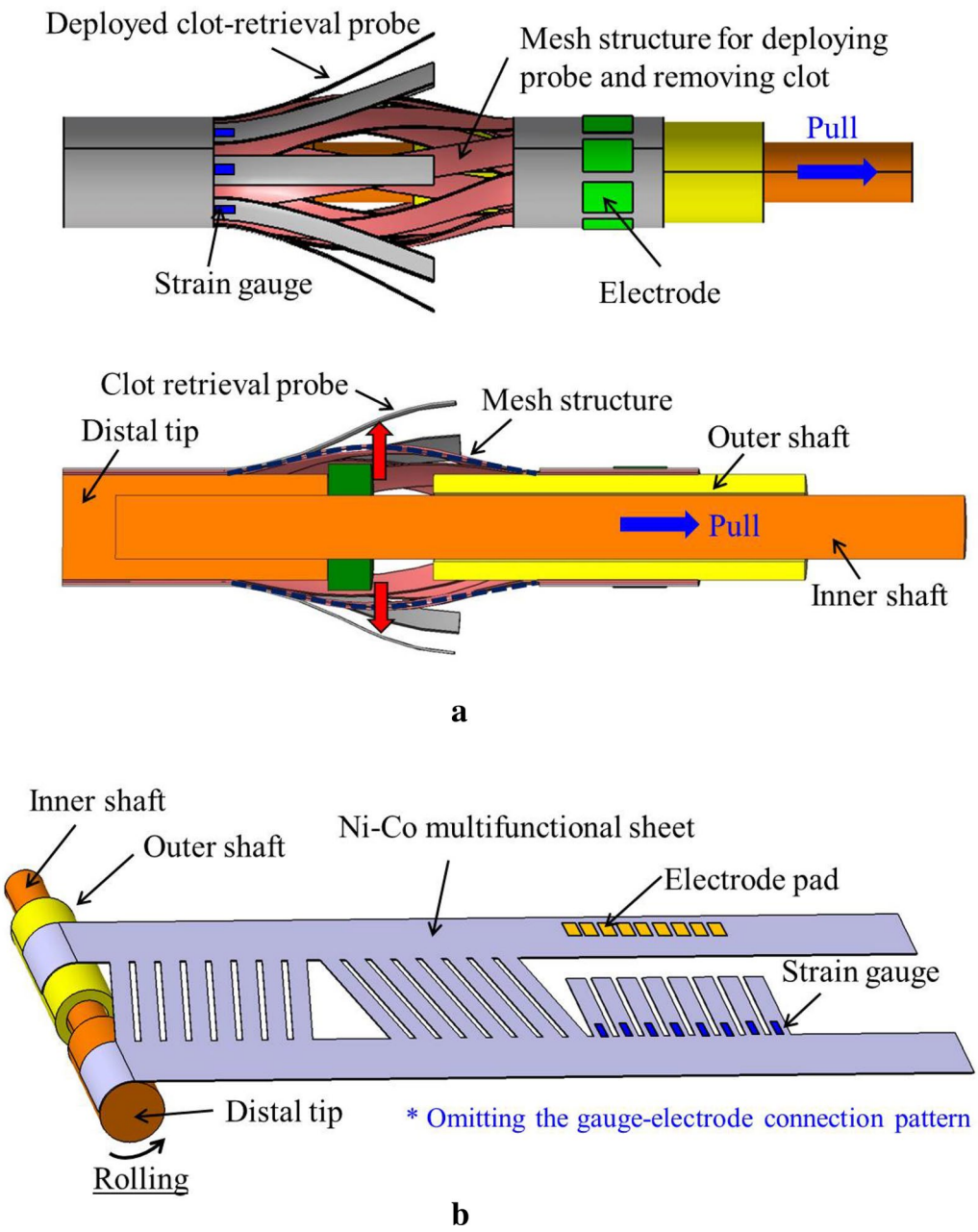

Fig. 1 **a** conceptual diagram of a MEMS-based smart catheter that enables the simultaneous diagnosis and treatment of vascular diseases, **b** schematic of the attachment process of the multifunctional sheet based on the Ni-Co flexible substrate for the realization of the smart catheter

bonding strength of the Pt strain gauges on the stainless-steel beam, through holes were formed in the Ni-Co substrate between the grids. The bonding strength can be improved by adhesive filling in the through holes.

Adhesion characteristics and cross-sectional structure

The scratch resistance and adhesion strength were evaluated using a nano-scratch tester (NST, CSM instruments). A sphero-conical diamond indenter with a radius of 2 μm was used for the scratch test. During the scratch test, the specimen was scratched with a ramping load that increased from 1 to 100 mN at a rate of 198 mN/min. The length of the scratching track was 0.1 mm. After the scratch test, the surface of the thin film was examined using an optical microscope. To evaluate the adhesion properties and scratch resistance of the Pt

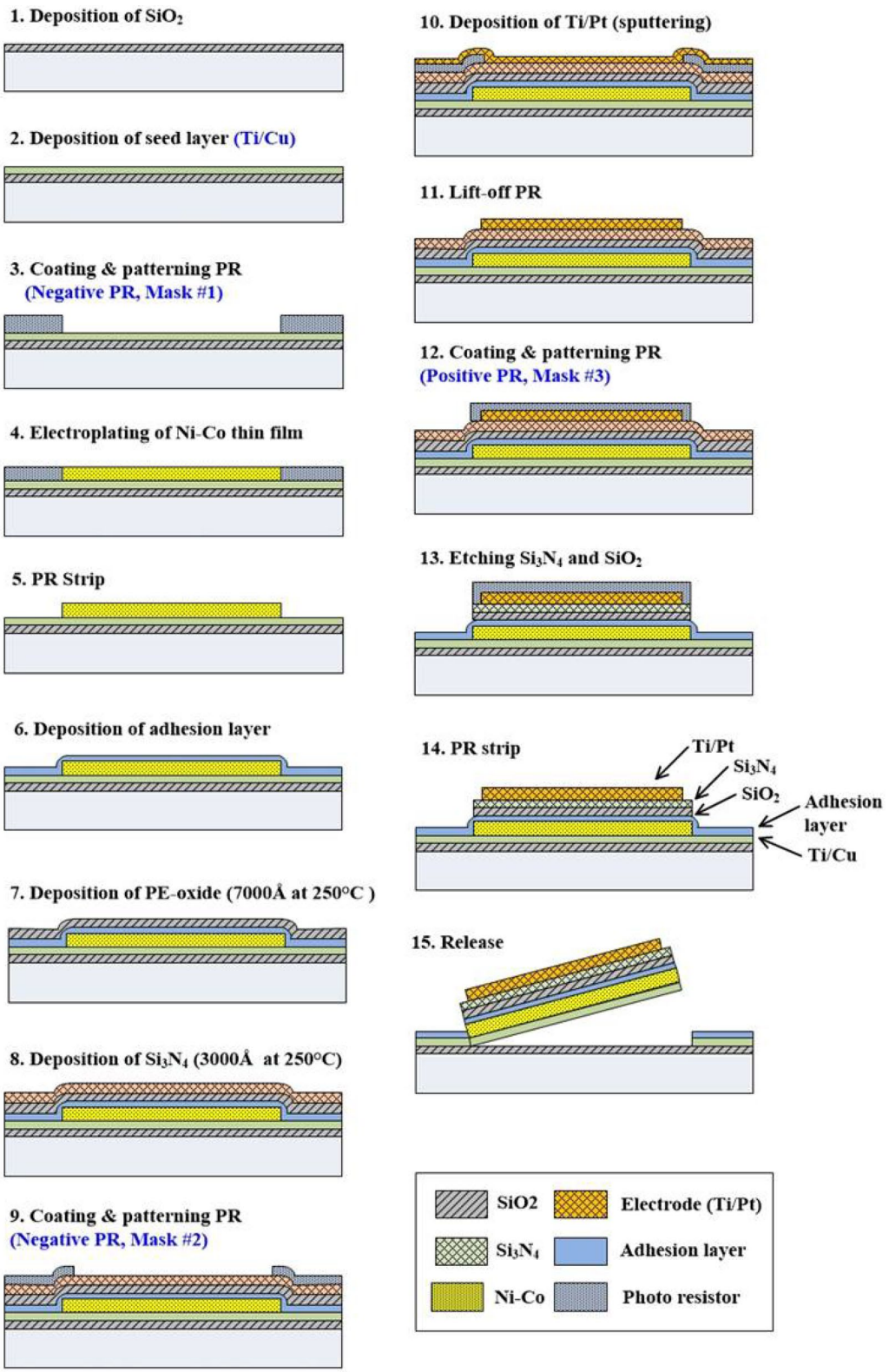

Fig. 2 Fabrication process of Pt strain gauges

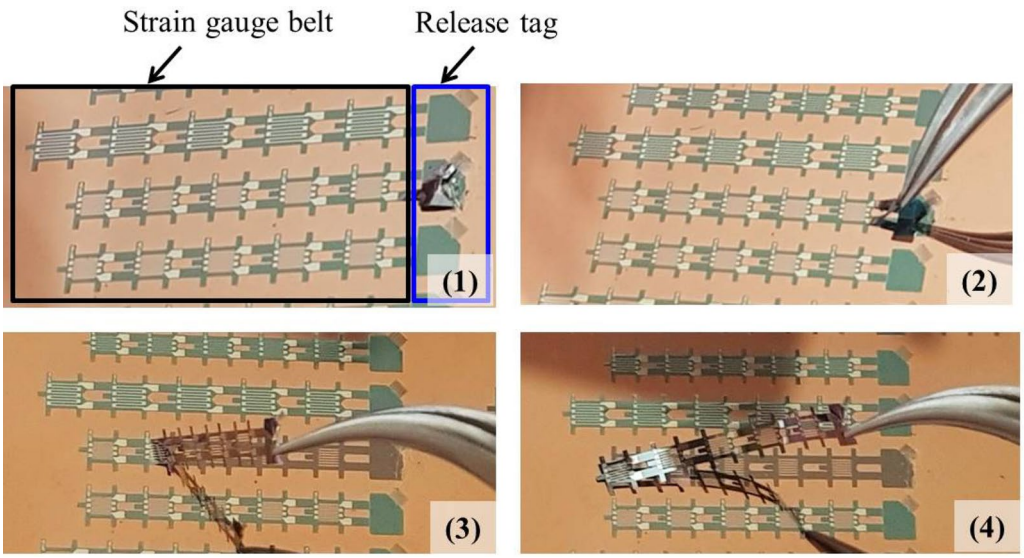

Fig. 3 Release process for Pt strain gauges

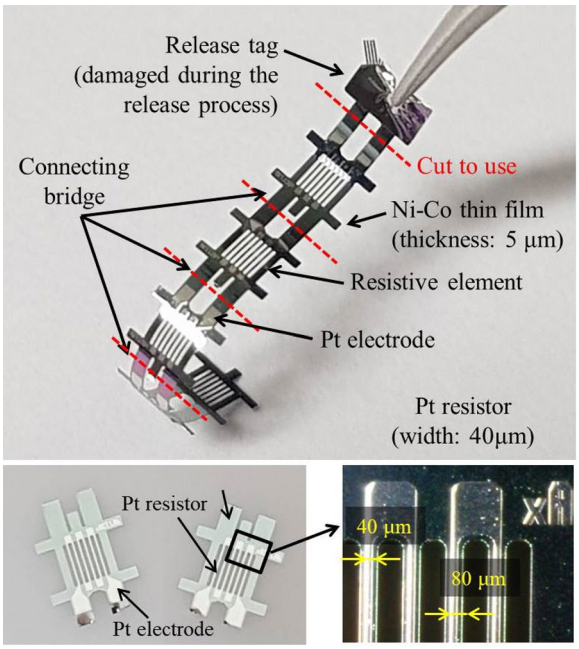

Fig. 4 Released Pt strain gauges

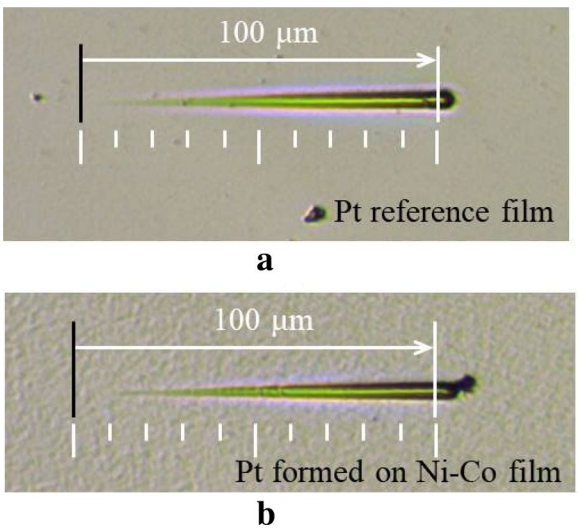

Fig. 5 Nano-scratch test results: **a** Pt reference film, and **b** Pt strain gauge based on Ni-Co flexible substrate

strain gauges based on the Ni-Co flexible substrate, the scratch test results of a reference film (where SiO_2 insulating layer and Ti/Pt metallization were sequentially deposited on silicon wafers) were compared to those of the Pt strain gauges.

The microscopic images of the thin films after the nano-scratch test are presented in Fig. 5. The microscopic image of the Pt reference film (Fig. 5a) reveals that the scratch trace of the reference film is initially smooth and shallow, and then gradually broadens and deepens with increasing load. As confirmed in the optical image, cracking and delamination did not occur during the scratch test; this implied that the film had good adhesion to the substrate. In Fig. 5(b), a microscopic image of the Pt strain gauge based on Ni-Co film is presented. In Fig. 5(b), there was nearly no scratch trace on the surface of the film at low loads. Similar to the reference Pt film, cracking and delamination were not observed, which indicated that the Pt strain

gauge developed in this study exhibited good adhesion strength to the substrate.

After cutting thin films through entire layers from the Ni-Co substrate to Pt metallization with precision medical scissors, the cross-sectional structure of the thin film was observed with SEM (SU8230, Hitachi). Figure 6 shows the SEM image of the cross section of the Pt Strain gauge. Although the film was cut with scissors, delamination did not occur. From the above results, it was concluded that the established fabrication process was valid.

Performance test of the Pt strain gauge

The Pt strain gauges formed on the probe made of Ni-Co are used to scan the inner geometries of the blood vessel, so the performance of the strain gauge in terms of gauge factor and nonlinearity should be investigated previously. For the performance test, the active and dummy strain gauges were bonded on the stainless-steel cantilever beam, and the printed circuit board (PCB) was attached near the strain gauge. The electrodes of the strain gauge and PCB were connected by wire-bonding.

The uniform strain distribution can be realized with the constant stress beam of the triangular shape [7], as shown in Fig. 7. The surface strain of the constant stress beam, ε, was calculated using Eq. (1):

$$\varepsilon = \frac{h}{L^2} \cdot \delta \tag{1}$$

Here, L, h, and δ denote the length from the fixed end to the deflected end, the beam thickness, and the endpoint deflection of the cantilever beam, respectively. In Eq. (1), the surface strain on the constant stress beam was uniform, regardless of the axial position.

The performance of the Pt strain gauges was evaluated using a quarter-bridge circuit consisting of two identical Pt stain gauges (active and dummy) and two fixed resistors, as shown in Fig. 8. At the initial condition, Pt strain gauges R_1 and R_2 and resistors R_3 and R_4 had equal resistance values.

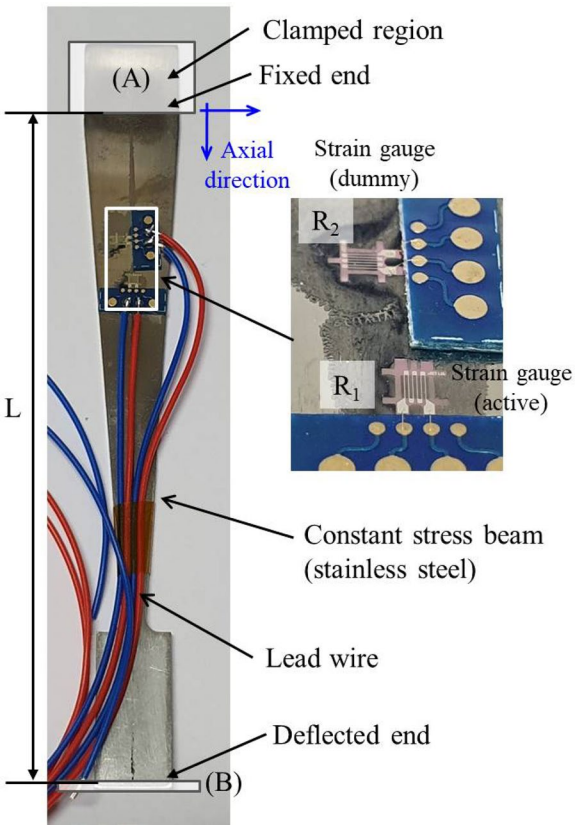

Fig. 7 Pt strain gauges bonded on the constant stress beam made of stainless steel

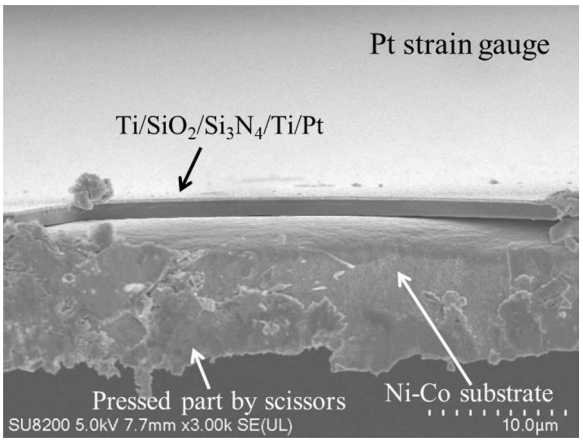

Fig. 6 SEM image of Pt strain gauge cross-section

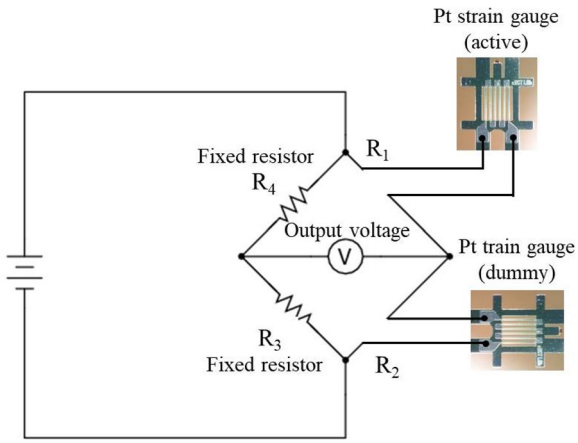

Fig. 8 Quarter bridge strain gauge circuit with temperature compensation

Figure 9 shows the experimental setup. The constant stress beam was mounted on points (A) and (B) of the performance test equipment. The endpoint of the cantilever beam was moved by a micrometer, and the corresponding deflection was measured by reading the gradation on the micrometer. The quarter-bridge circuit was supplied with an excitation voltage of 5 V using a power supply (OPM-303D, ODA), and the output voltage was measured with a digital multimeter (8846A, Fluke).

The ratio of the excitation and output voltages was calculated using Eq. (2) as follows:

$$\frac{V_{out}}{V_{exc}} = \frac{1}{4}\left(\frac{\Delta R_1}{R_1} - \frac{\Delta R_2}{R_2} + \frac{\Delta R_3}{R_3} - \frac{\Delta R_4}{R_4}\right) \tag{2}$$

Here, GF, R_1, R_2, R_3, and R_4 denote the gauge factor of the Pt strain gauge and resistance values of resistors 1, 2, 3, and 4, respectively. In this study, ΔR_3 and ΔR_4 were zero, regardless of the load applied to the cantilever beam, because resistors 3 and 4 were fixed resistors. ΔR_1 varied with temperature as well as physical strain, while ΔR_3 merely varied with temperature. Moreover, the initial resistance values of resistors 1 and 2 were the same, so R_1 equaled R_2. Thus, it was possible to express Eq. (2) as Eq. (3):

$$\frac{V_{out}}{V_{exc}} = \frac{1}{4}\left(\frac{\Delta R_\varepsilon - \Delta R_T}{R} - \frac{\Delta R_T}{R}\right) = \frac{\Delta R_\varepsilon}{4R} \tag{3}$$

The gauge factor, which is the ratio between the relative change in electrical resistance and the mechanical strain, indicates the sensitivity of a strain gauge and was calculated using Eq. (4):

$$GF = \frac{\Delta R_\varepsilon / R}{\varepsilon} \tag{4}$$

Thus, Eq. (3) was simplified to Eq. (5):

$$\frac{V_{out}}{V_{exc}} = \frac{GF}{4} \cdot \varepsilon \tag{5}$$

Substituting Eq. (1) into Eq. (5) yielded Eq. (6):

$$\frac{V_{out}}{V_{exc}} = \frac{GF \cdot h}{4L^2} \cdot \delta \tag{6}$$

The gauge factor of the Pt strain gauge was calculated by measuring the output voltage and deflection at the end of the cantilever beam. L and h were 100 mm and 1.0 mm, respectively.

In this study, the nonlinearity of the Pt strain gauges was evaluated. Nonlinearity refers to the maximum deviation of the actual value from the best-fitting straight line through the points and was calculated using Eq. (7) as follows:

$$\text{Nonlinearity} = \frac{R_{fit} - R_{act}}{R_{max} - R_{min}} \tag{7}$$

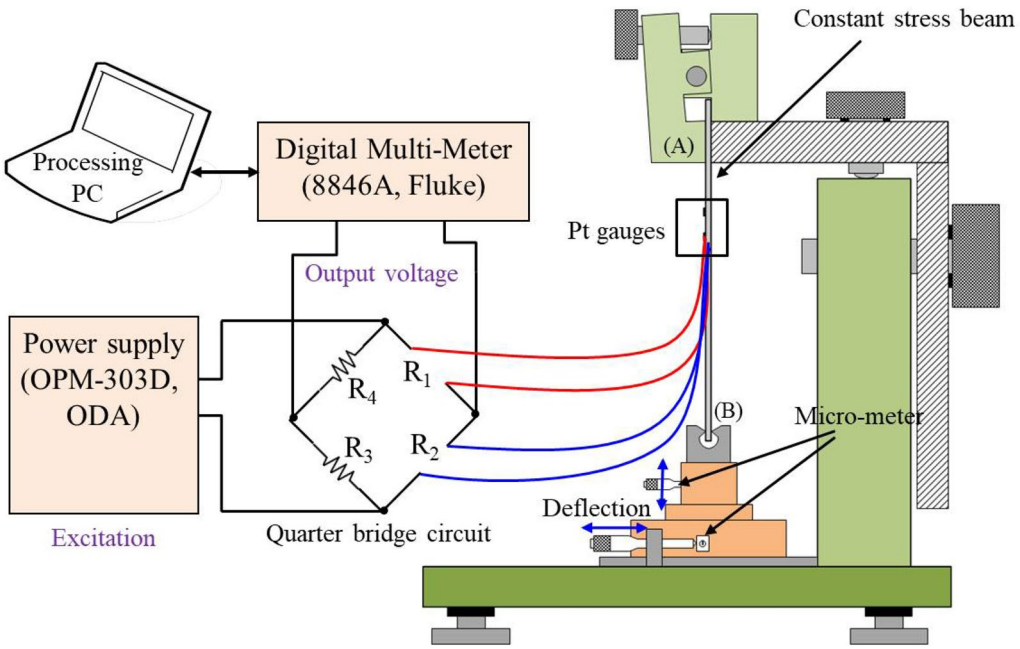

Fig. 9 Experimental setup for performance test of Pt strain gauges

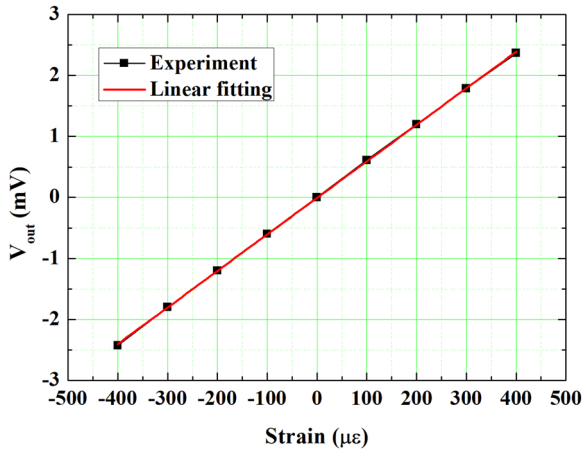

Fig. 10 Output voltage of Pt strain gauge as a function of strain at room temperature

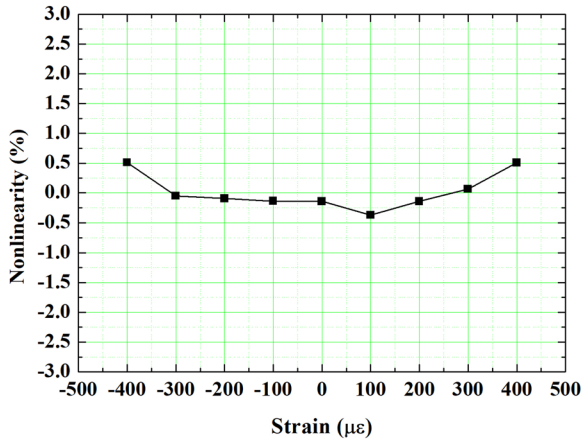

Fig. 11 Nonlinearity of Pt strain gauge as a function of strain

Here, R_{act} is the actual resistance at strain ε, and R_{fit} is the resistance from the straight line that is curve-fitted with the actual upper value R_{max} and lower value R_{min} at strain ε.

Results and discussion

Figure 10 shows the output voltage as a function of the strain calculated using Eq. (1). The output voltage increased linearly as the strain gauge was deformed by tensile stress, while it decreased with the application of compressive stress. The gauge factor of the Pt strain gauge based on the Ni-Co flexible substrate was calculated using Eq. (5), and the value was 4.8. This value was slightly higher than the gauge factor (approximately 3.8) of the Pt strain gauge reported by other researchers [8, 9], about 2.3 times larger than that of the commercial metal foil strain gauge (approximately 2.1), and approximately 2.4 to 3.4 times larger than the gauge factor (1.4 ~ 2.0) of the metal silicate strain gauge [10].

In Fig. 10, the red line indicates the best-fitting straight line through the points. The actual data followed the value of the fitted line, corresponding to the strain. Figure 11 shows the degree of nonlinearity as a function of strain at room temperature. Nonlinearity resulted in a maximum value of 0.5% FS at the maximum and minimum strains, corresponding to 400 and -400 μm. Considering that the nonlinearity value of the general commercial strain gauge was approximately 0.3% or less, the nonlinearity of the Pt strain gauge developed in this study was slightly higher than that of the commercial strain gauge. This was due to the weak adhesion strength of the adhesive. We used a medical grade adhesive (AC-526 N, EpoxySet) to bond the Pt strain gauge on the stainless-steel beam. When the high strains were applied to the Pt strain gauges, the adhesive could not maintain the bonding between the stainless-steel beam and the Pt strain gauges because of the very high stiffness of the Ni-Co substrate. As a result, the maximum nonlinearity occurred in the section where the deformation was significantly applied. Degradation of nonlinearity due to the weak bonding strength of the organic adhesives was not expected to occur in the design of the smart catheter proposed in this paper because the Pt resistors were embedded on the Ni-Co flexible structures.

Figure 12 shows a micro-probe sensor for application to smart catheters using Pt strain gauges developed in this study. In order to form quarter-bridge strain gauge circuit with temperature compensation [10], active and dummy Pt strain gauges are placed on the micro probe sensor. It was confirmed that the Ni-Co flexible substrate can be patterned into a very complex shape without any damages. Moreover, the micro-probe sensor can be peeled off from the Si carrier wafer and attached to structural element in other electromechanical systems; even it can be attached to a curved surface. The electrodes of the micro-probe sensor will be connected by wire-bonding to flexible PCB.

Conclusion

In this study, the design of a MEMS-based smart catheter that enables the simultaneous diagnosis and treatment of vascular diseases is proposed. For the design of the smart catheter, Pt strain gauges were formed on a flexible micro probe made of Ni-Co to scan the inner shape of the blood vessels and retrieve the blood clots. Ni-Co thin films were used not only as substrates, but also as structural elements.

As a preliminary study, a new fabrication process for Pt strain gauges based on a Ni-Co flexible substrate was

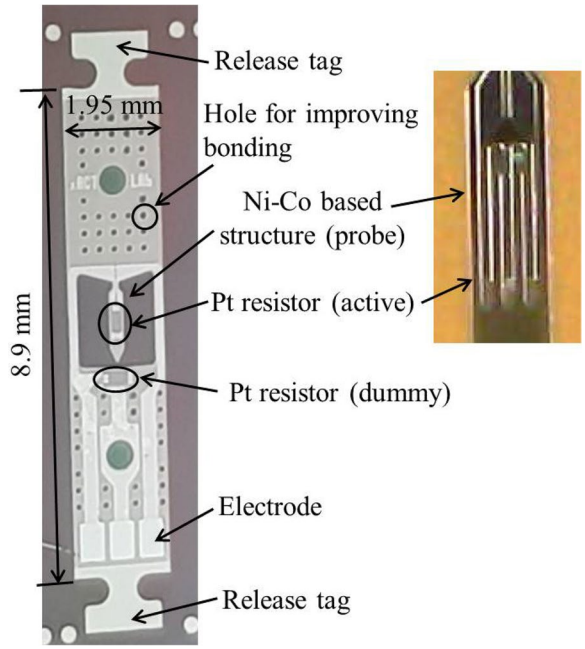

Fig. 12 Micro-probe sensor for application to smart catheters using Pt strain gauges developed in this study

established, and its performance in terms of gauge factor and nonlinearity was evaluated. During the fabrication process, the Ni–Co thin film was deposited and patterned on a Si carrier wafer using the conventional electroplating process, and multilayered Pt resistors were formed thereon. Afterward, the Pt strain gauge belt was peeled-off from the Si carrier wafer with a new release process using the release tag formed at the end of the Pt strain gauge belt. Following this fabrication process, flexible microdevices with a thickness of several micrometers and significantly complex shape can be easily realized.

Because the Pt strain gauges were composed of a multilayered thin film in which adhesion, insulating, and Pt layers were formed on the Ni-Co substrate, the adhesion strength of the thin films was investigated using a nano-scratch test. The experimental results of the nano-scratch test indicated that cracking and delamination did not occur, and that the film had good adhesion to the substrate.

The Pt strain gauges were bonded to a constant stress beam made of stainless steel, and a performance test was carried out. The results of the performance test revealed that the output voltage changed in proportion to the deformation applied to the strain gauge, and the gauge factor showed a value of 4.8. As a result of measuring nonlinearity, the values of 0.5% FS were determined to be available as sensors, because these values were within 1%.

For future work, the fabrication process established in this study will be used to realize MEMS-based smart catheters as well as other flexible micro devices such as electrothermal actuators, multifunctional metamaterials, energy harvesting devices, sensors, and micro mirrors.

Acknowledgements
We thanks to members of our laboratory (xACT Lab.) for sincere comments on this research.

Authors' contributions
YK and JK conducted the main experiment. YK supervised the project. All authors read and approved the final manuscript.

Funding
This study was conducted with the support of the Korea Science and Engineering Foundation through the funding of the Ministry of Education, Science, and Technology in 2020 (NRF-2019R1F1A1060772).

Availability of data and materials
All data generated or analyzed during this study are included in this published article.

Competing interests
The authors declare no competing interests (both financial and non-financial).

Received: 29 June 2020 Accepted: 3 August 2020
Published online: 11 August 2020

References

1. Fred K. Nakhjavan (1998) Catheter for removal of clots in blood vessels, US Patent 5772674A, 30 June 1998
2. Scott L. Jahrmarkt (2018) Guidewire and catheter system and method for treating a blood clot, US Patent 9943668B2, 17 April 2018
3. Eran Levit, Eran Hirszowicz, Maurice Buchbinder (2013) Balloons and Balloon Catheter Systems for Treating Vascular Occlusions. US8372034B2, US patent, 2013.02.12
4. Thomas V Ressemann, Steven S Hackett, Andrew J Dusbabek, Dennis W Wahr (2009) Emboli Protection Devices and Related Methods of Use. US Patent 7604612B2, 20 October 2009
5. Yongdae Kim (2020) Catheter Capable of Diagnosing and Treating Vascular Diseases. KOR Patent 10-2020-0002481, 08 January 2020
6. Yongdae Kim, Gap Seop Sim, and Kwang-Seop Kim (2019) Fabrication Process and Mechanical Properties of Ni-Co Thin Films and Fabrication Results of the Flexible MEMS Device Formed on the Ni-Co Substrate. Paper presented at the 2019 KMEMS conference, Jeju KAL hotel, 2019
7. Yongdae Kim (2010) MEMS Thin Silicon Gauge for Strain Measurement of Structural Elements. Dissertation, KAIST
8. Soeren Fricke, Alois Friedberger, Gerhard Mueller, Helmut Seidel, and Ulrich Schmid (2008) Strain gauge factor and TCR of sputter deposited Pt thin films up to 850°C. Paper presented at the IEEE SENSORS 2008, Lecce, Italy, 26-29 October 2008
9. Schmid P, Zarfl C, Balogh G, Schmid U (2014) Gauge factor of titanium/platinum thin films up to 350°C. Procedia Engineering 87:172–175
10. Beeby S, Ensell G, Kraft M, White N (2004) MEMS Mechanical Sensor. Artech House, Norwood

Publisher's Note